ADVANCED MATERIALS

Supporting Information

for *Adv. Mater.*, DOI: 10.1002/adma.201305241

Core-Sheath Carbon Nanostructured Fibers for Efficient Wire-Shaped Dye-Sensitized Solar Cells

*Xin Fang, Zhibin Yang, Longbin Qiu, Hao Sun, Shaowu Pan, Jue Deng, Yongfeng Luo, and Huisheng Peng**

Supporting Information

Experimental Section

(1) Preparation of CNT fibers

CNT fibers were dry-spun from spinnable CNT arrays. The CNT arrays were synthesized by chemical vapor deposition at 750 ℃ with Fe (1.2 nm)/Al_2O_3 (5 nm) on a silicon wafer as catalyst, C_2H_4 (90 sccm) as carbon source, a mixture of Ar (480 sccm) and H_2 (30 sccm) as carrier gas. The resulting CNT array was ~240 μm in height. CNT fibers were then spun from the array with a rotation speed of 2000 rpm. The diameter of the fiber was ~ 20 μm and several meters in length.

(2) Fabrication of stretchable wire-shaped DSCs

An elastic fluororubber fiber with diameter of 1 mm was first wrapped with CNT sheets. The resulting fiber was then treated in a mixture of 50 mL of concentrated H_2SO_4 and 50 mg of $KMnO_4$ at 75−80 ^oC for 1−2 hr. The treated fiber was further washed with deionized water and subsequently reduced in HI solution at 80 ^oC for 8 hr, followed by washing with deionized water and drying for 12 hr in air. A Ti solenoid was made by intertwining a Ti wire (diameter of 127 μm) around a steel rod with diameter of 1.25 mm. The Ti solenoid was then modified with perpendicularly aligned TiO_2 nanotubes on the surface by the same procedures described in the main text. Finally, the stretchable rubber fiber and modified Ti solenoid were assembled together and sealed within a stretchable tube, followed by injection of the electrolyte.

(3) Characterization

The structures were characterized by TEM (JEOL JEM-2100F operated at 200 kV), SEM (Hitachi FE-SEM S-4800 operated at 1 kV), and AFM (SHIMADZ SPM-9500J3). Raman spectra were obtained from LabRam-1B with an excitation wavelength of 633 nm and laser power of 4 mW. The cyclic voltammetry was performed in a three-electrode system on CHI 660 electrochemical workstation at room temperature with Pt wire and Ag/AgCl as counter and reference electrodes, respectively. The electrolyte included an acetonitrile solution containing 5 mM LiI, 0.5 mM I_2, and 0.05 M $LiClO_4$. Stress-strain curves were made from the Shimadzu Table-Top Universal Testing Instrument. J-V curves were recorded by a Keithley 2400 Source Meter under illumination (100 mW/cm^2) of simulated AM 1.5 solar light coming from a solar simulator (Oriel-Sol3A 94023A equipped with a 450 W Xe lamp

and an AM 1.5 filter). The electrochemical impedance spectroscopy was performed on CHI 660a electrochemical workstation in dark.

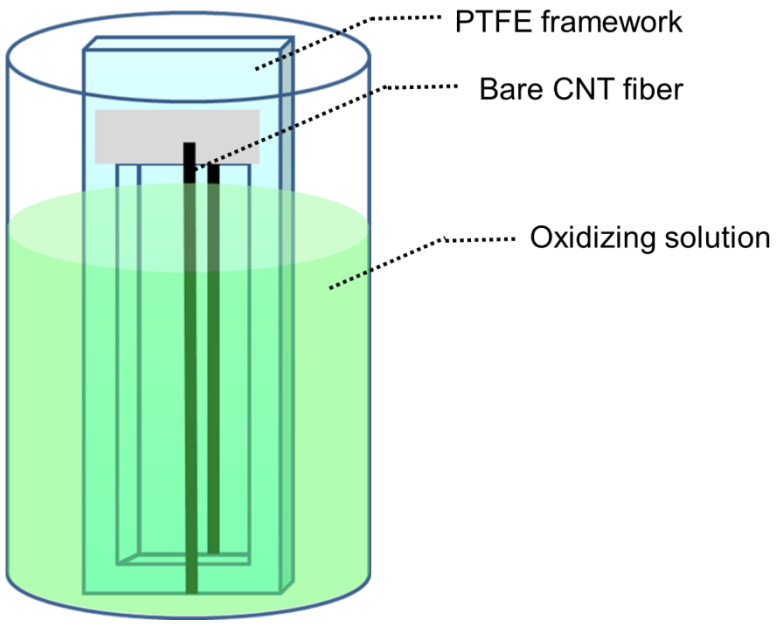

Figure S1. Schematic illustration to the experimental setup for the oxidation of CNTs. A fiber was bound onto a PTFE framework and immersed into the oxidizing solution.

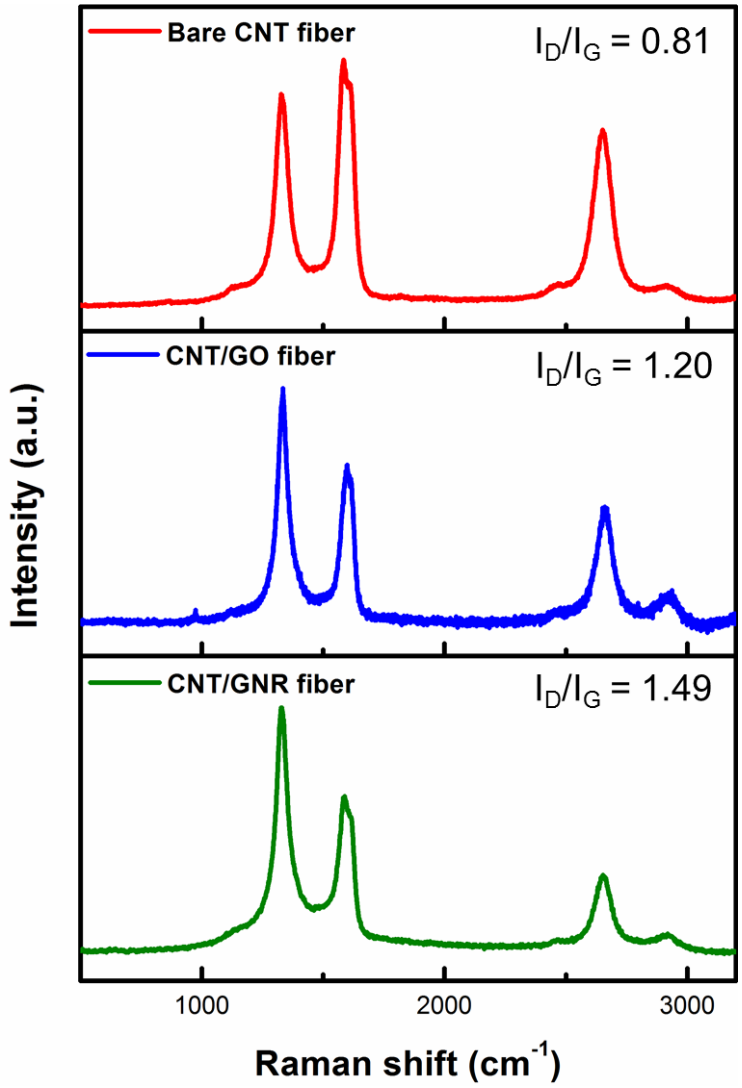

Figure S2. Raman spectra of the bare CNT fiber, CNT/GO fiber and CNT/GNR fiber.

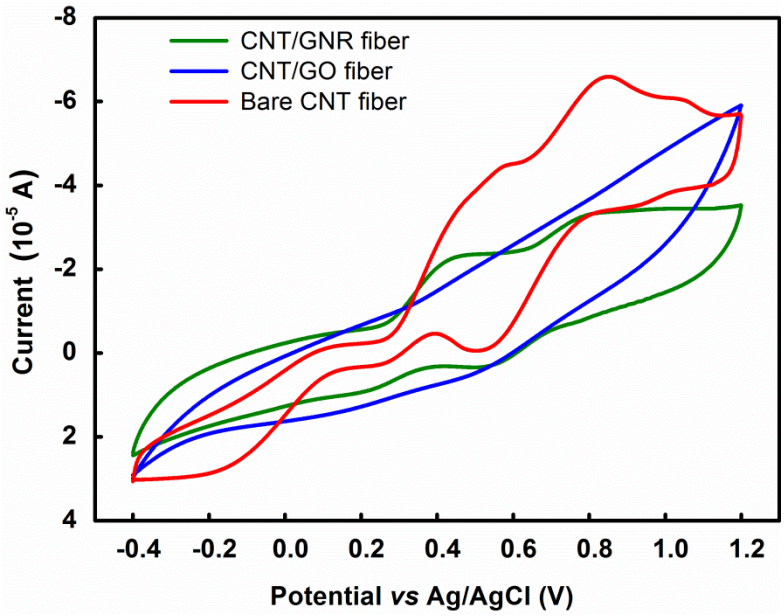

Figure S3. Cyclic voltammograms for the bare CNT fiber, CNT/GO fiber, and CNT/GNR fiber in I_3^-/I^- redox system.

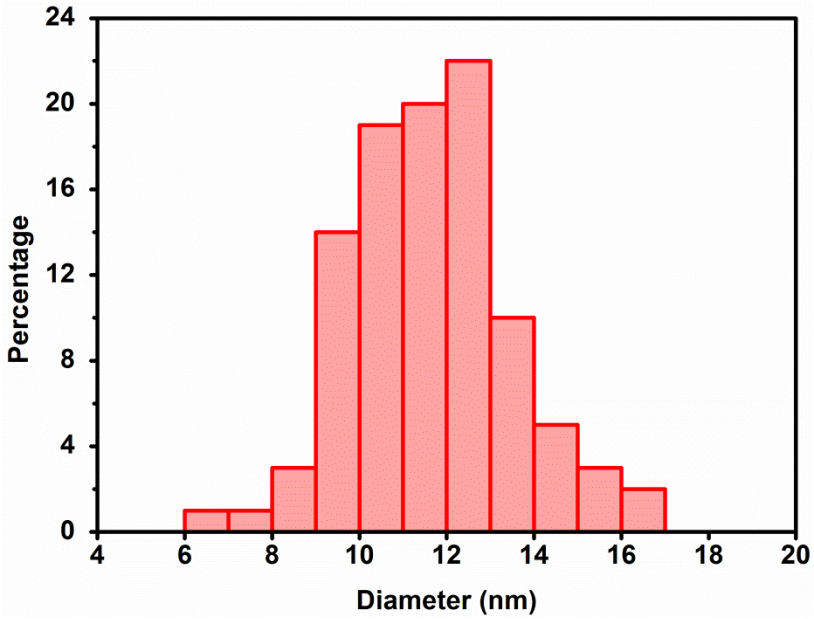

Figure S4. Diameter distribution of CNTs.

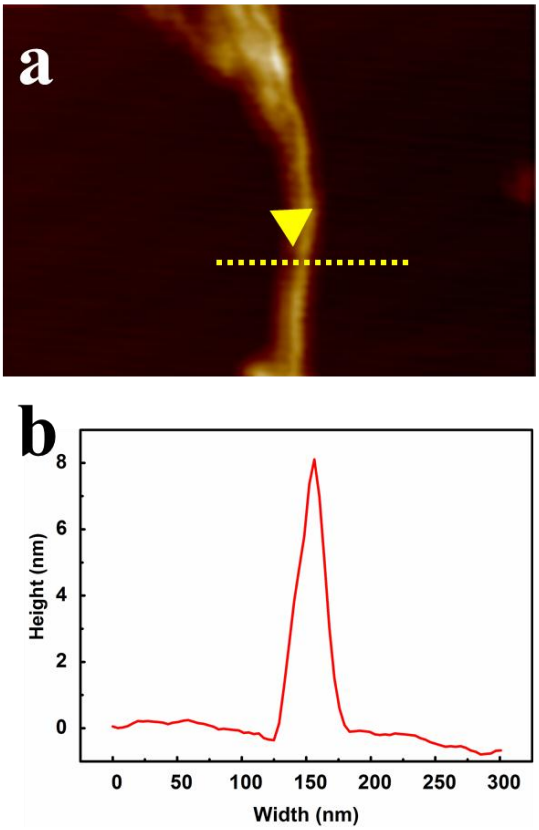

Figure S5. a. AFM image of CNTs. **b.** Height graph of a CNT.

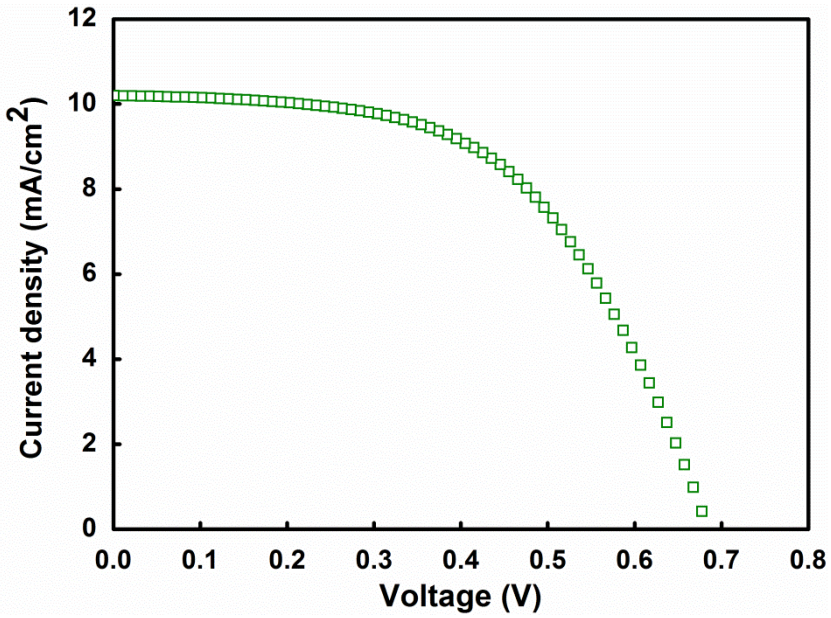

Figure S6. J-V curve of wire-shaped DSCs with the HI-treated CNT fiber as the counter electrode.

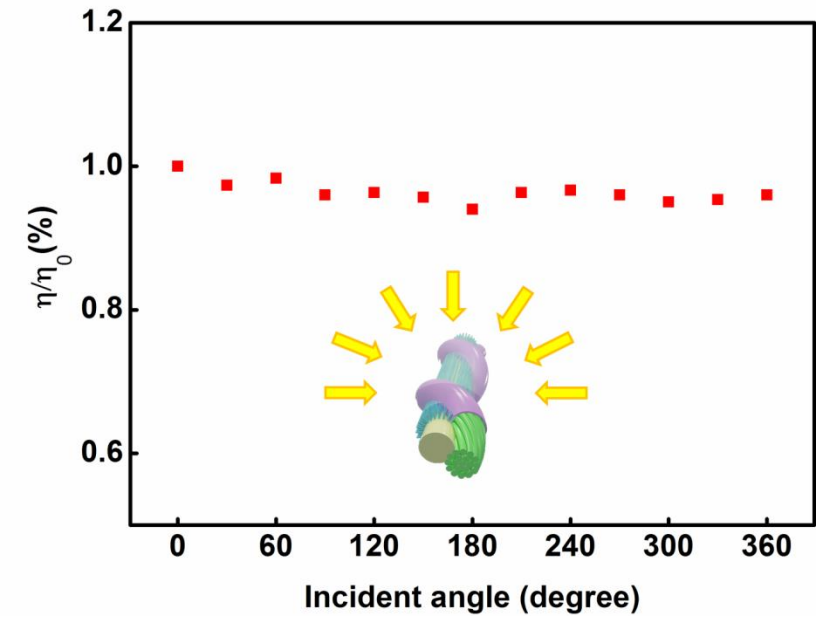

Figure S7. Dependence of energy conversion efficiency on incident angle for a wire-shaped DSC. η_0 and η correspond to the energy conversion efficiencies measured at an incident angle of 0^o and other angles, respectively.

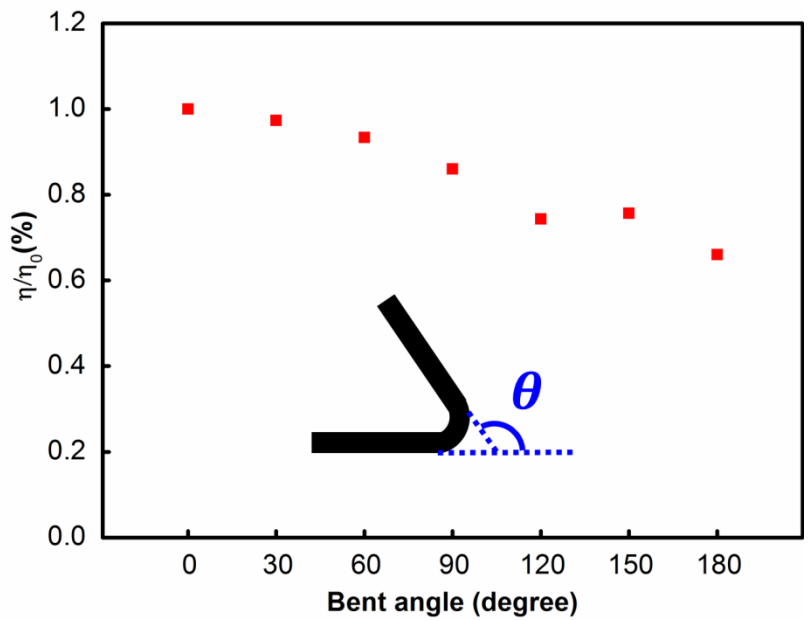

Figure S8. Dependence of energy conversion efficiency on bent angle for a wire-shaped cell. η_0 and η correspond to the energy conversion efficiencies measured at a bent angle of 0^o and the other angles, respectively.

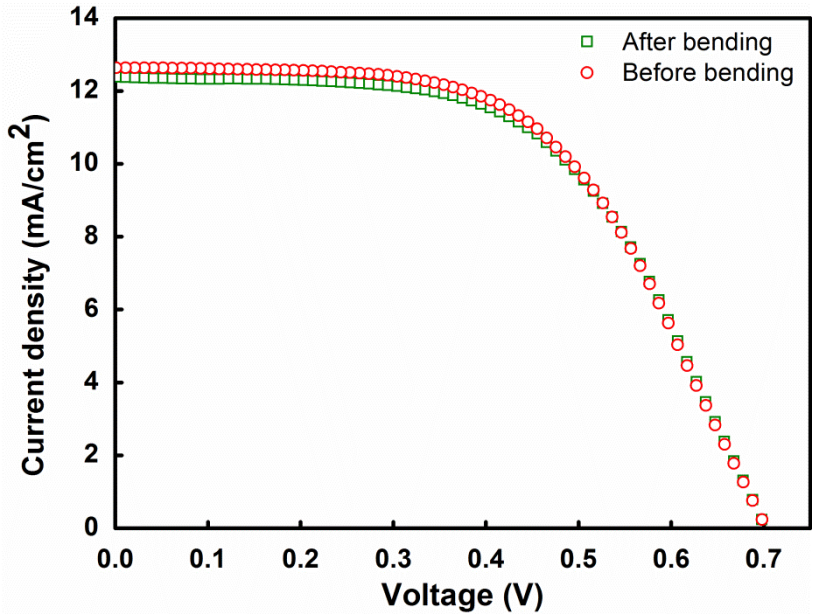

Figure S9. J-V curves of a wire-shaped DSC before and after bending to 90 ^{o}.

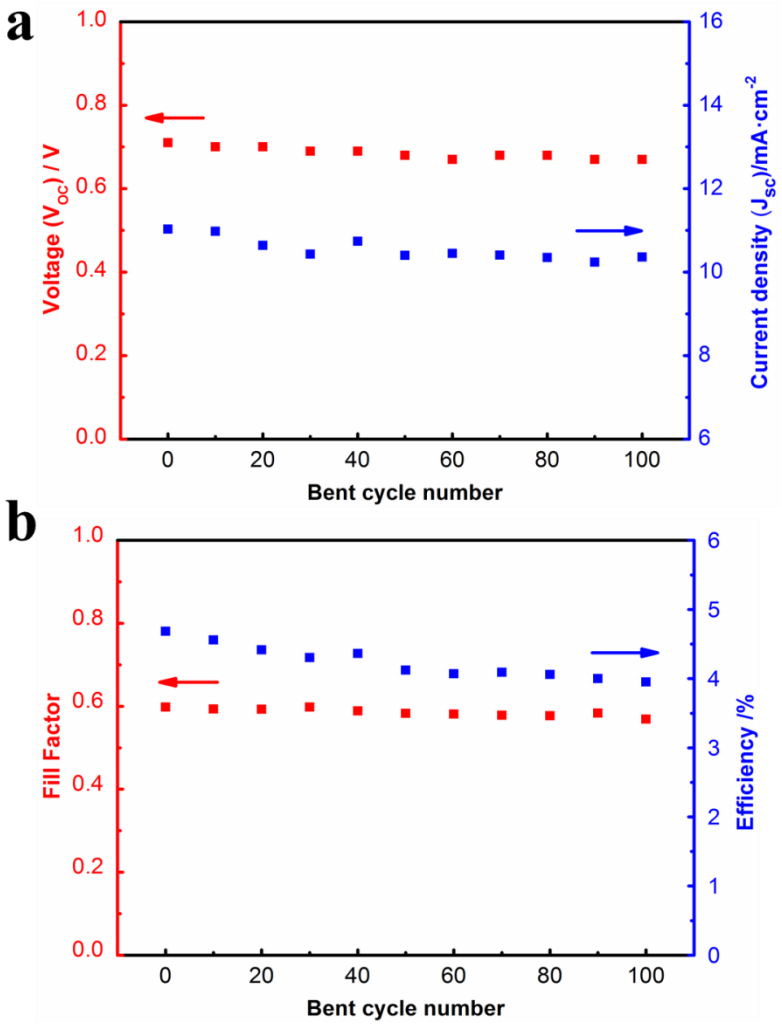

Figure S10. Photovoltaic parameters of a wire-shaped DSC before and after bending up to 100 cycles.

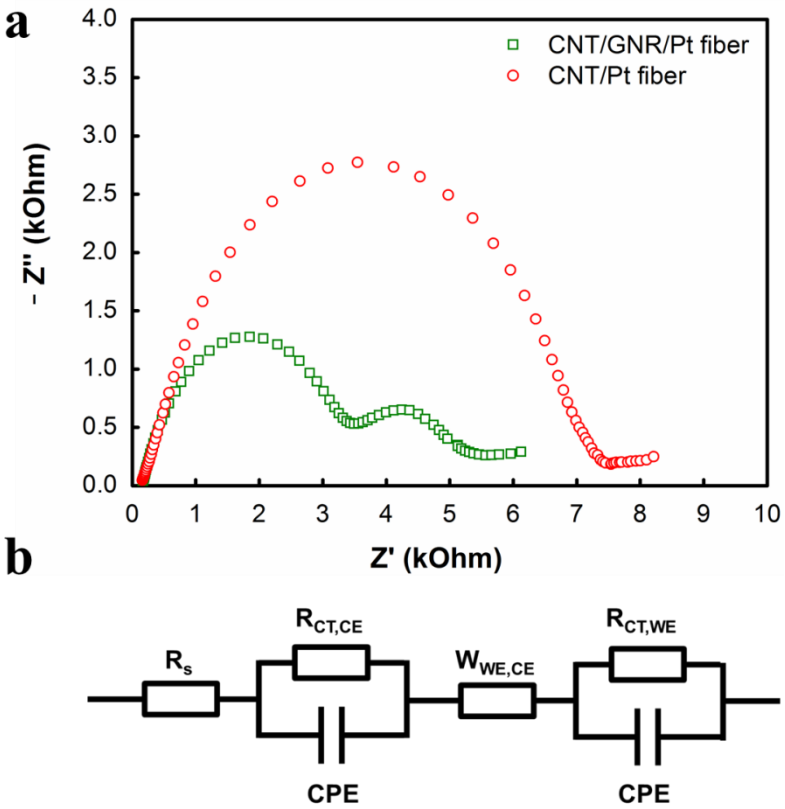

Figure S11. a. Electrochemical impedance spectra of wire-shaped DSCs with different counter electrodes deposited with Pt nanoparticles. **b**. Equivalent circuit for wire-shaped DSCs with R_S, $R_{CT,CE}$, $R_{CT,WE}$, $W_{WE.CE}$, and CPE as serial resistance, charge-transfer resistance at counter electrode, charge-transfer resistance at TiO_2/electrolyte interfaces, electrolyte diffusion impedance, and constant phase element, respectively.

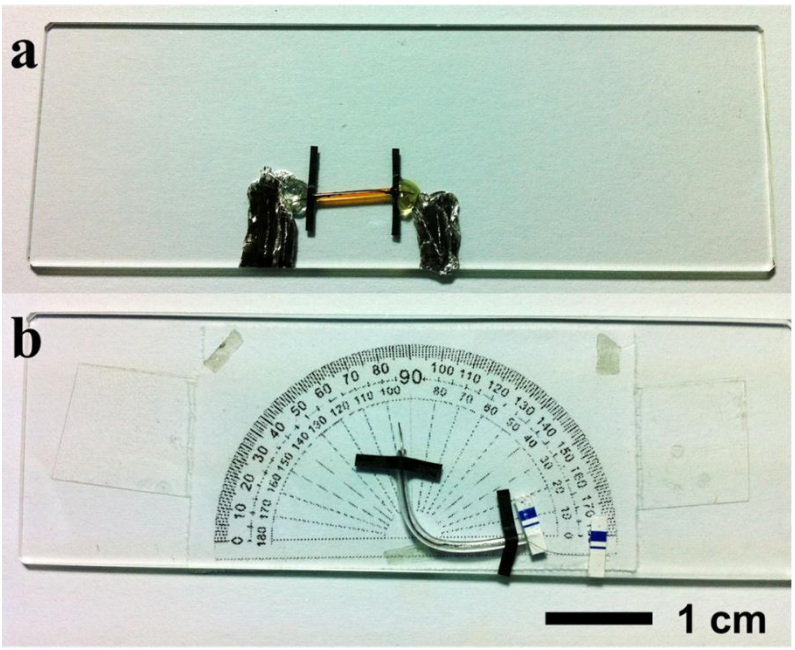

Figure S12. Photographs of wire-shaped DSCs encapsulated in a capillary tube (**a**) and flexible fluorinated ethylene propylene tube (**b**).

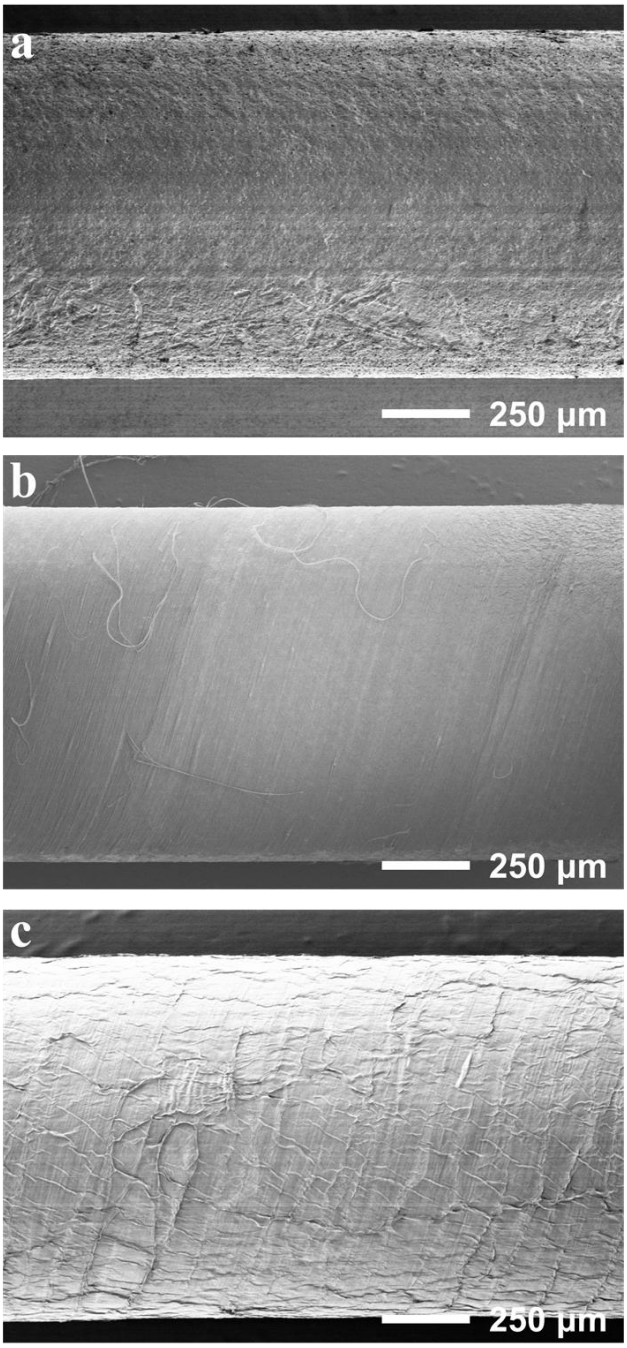

Figure S13. SEM images. **a** and **b.** An elastic rubber before and after wrapped with CNT sheets, respectively. **c.** The CNT-wrapped fiber after chemical treatment.

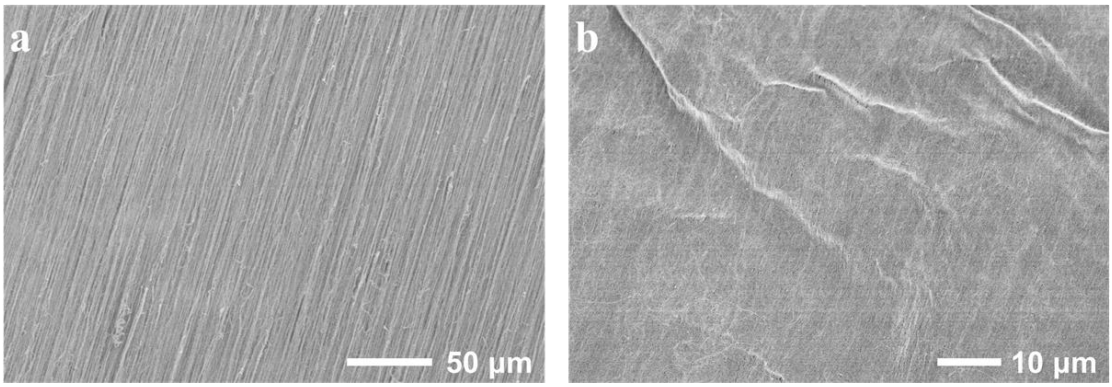

Figure S14. SEM images. **a.** The wrapped CNT sheet. **b**. The formed GNR sheath by unzipping the CNT.

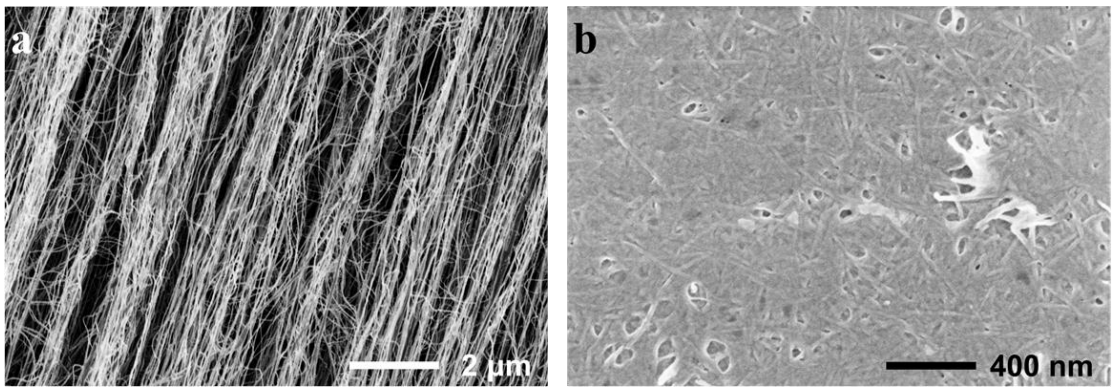

Figure S15. SEM images at high magnifications. **a.** The wrapped CNT sheet. **b**. The formed GNR sheath by unzipping the CNT.

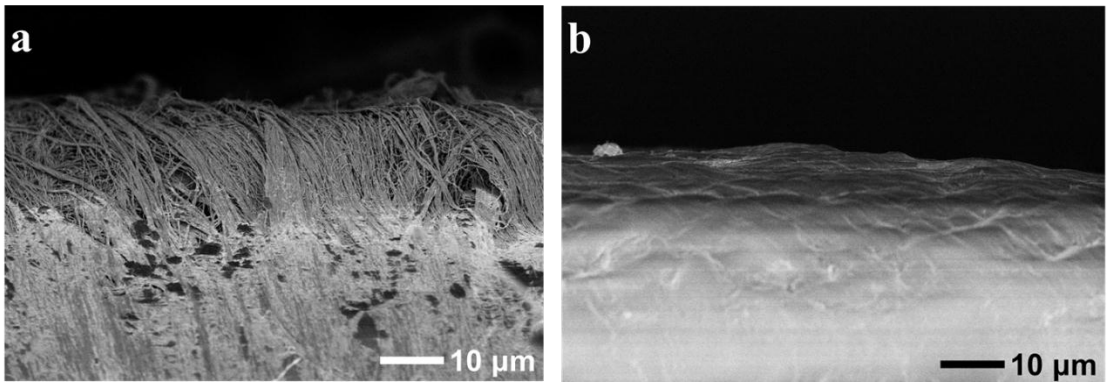

Figure S16. Cross-sectional SEM images. **a.** The wrapped CNT sheet. **b**. The formed GNR sheath by unzipping the CNT.

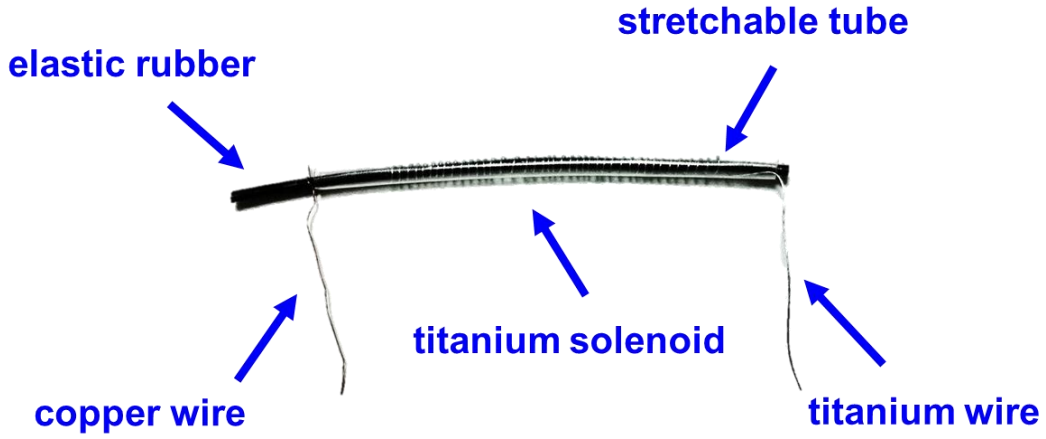

Figure S17. Photograph of a stretchable wire-shaped DSC.

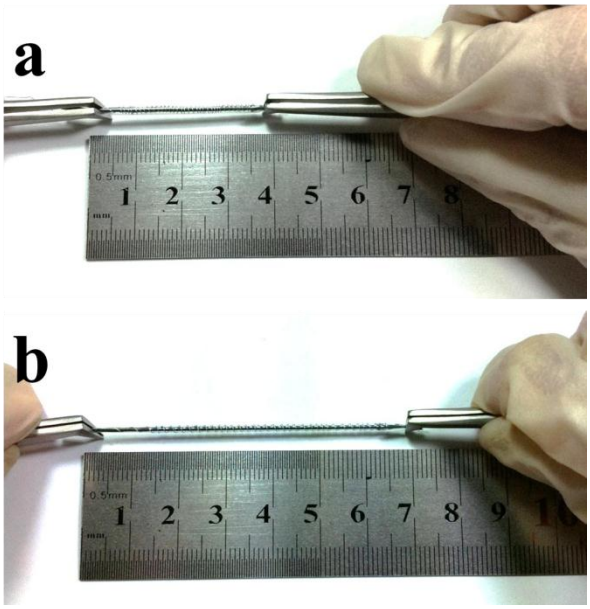

Figure S18. Photographs of a stretchable DSC before and after being stretched by 100%, respectively.

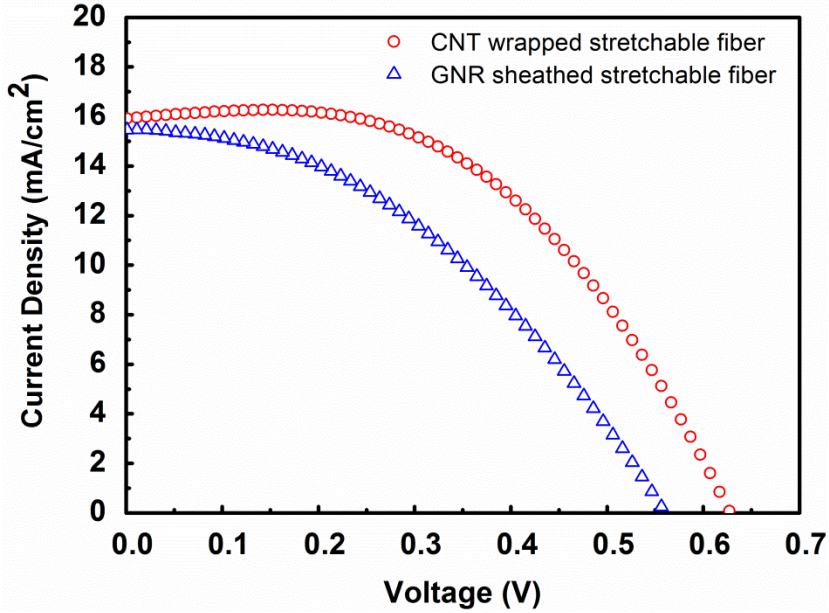

Figure S19. J-V curves of stretchable wire-shaped DSCs based on the stretchable fibers with the CNT sheet (red circle) and GNR layer (blue triangle) in the sheath as counter electrodes.

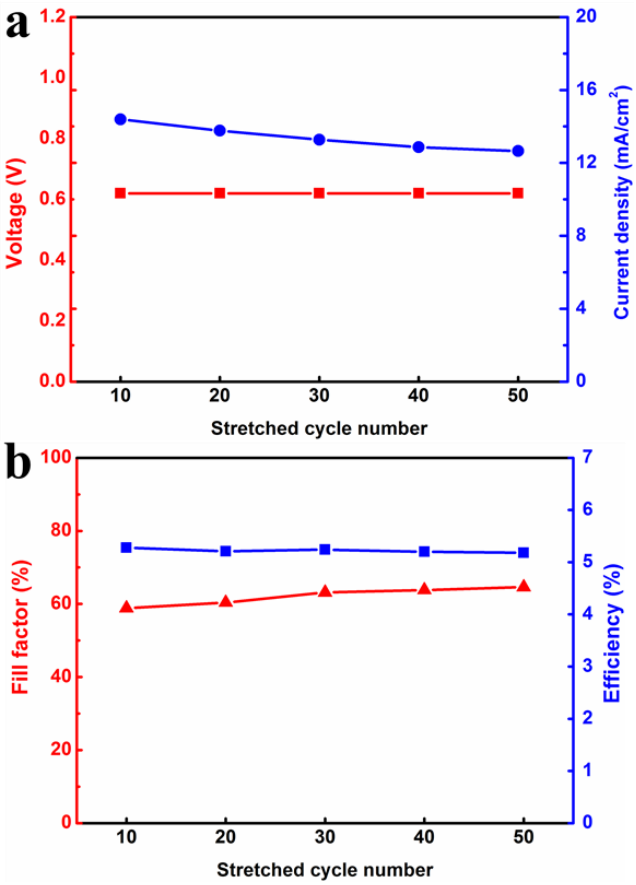

Figure S20. Dependence of the photovoltaic parameter of the stretchable DSC on the stretched cycle.